Supporting Information

Ru Nanoparticles Supported on $Mg(OH)_2$ Microflowers as Catalysts for Photothermal Carbon Dioxide Hydrogenation

Ning Kong,[†] Bin Han,[‡] Zhao Li,[†] Yaosi Fang,[†] Kai Feng,[†] Zhiyi Wu,[†] Shenghua Wang,[†] Ao-Bo Xu,[†] Yingying Yu,[†] Chaoran Li,[†,] Zhang Lin[‡,*] and Le He[†,*]*

[†]Institute of Functional Nano & Soft Materials (FUNSOM), Jiangsu Key Laboratory for Carbon-Based Functional Materials & Devices, Soochow University, Suzhou, Jiangsu 215123, China

[‡]School of Environment and Energy, Key Laboratory of Pollution Control and Ecosystem Restoration in Industry Clusters (Ministry of Education), Guangdong Engineering and Technology Research Center for Environmental Nanomaterials, South China University of Technology Guangzhou, 510006, China

E-mails: lehe@suda.edu.cn, zlin@scut.edu.cn, crli@suda.edu.cn.

KEYWORDS: photothermal catalysis, CO_2 hydrogenation, strong light absorption, solar-to-fuel conversion, ion-exchange strategy

1 Experimental Section

1.1 Chemicals

All reagents were used as received without further purification. Magnesium sulfate heptahydrate ($MgSO_4 \cdot 7H_2O$, AR) and ethanol absolute (C_2H_6O, GR) were purchased from Sinopharm Chemical Reagent Co. Ltd. (Shanghai, China). Ruthenium chloride hydrate ($RuCl_3 \cdot xH_2O$) and ammonium hydroxide solution ($NH_3 \cdot H_2O$, 28 wt%) were obtained from Aladdin and Macklin, respectively. Milli-Q water (Millipore, 18.2 MΩ cm at 25 °C) was used in all experiments.

1.2 Synthesis of $Mg(OH)_2$ nanoflowers.

12.3 g of $MgSO_4 \cdot 7H_2O$ was dissolved in 25 mL of deionized water. The resulting transparent solution was heated at 60°C under magnetic stirring. Then 15 mL of $NH_3 \cdot H_2O$ was added to the above solution. After being cooled to room temperature, the white products were collected through centrifugation, washed with ethanol for three times, and dried at 80 °C in a vacuum oven.

1.3 Synthesis of $Mg(OH)_2$ supported Ru catalysts.

200 mg of the as-obtained $Mg(OH)_2$ nanoflowers was dispersed in 20 mL of ethanol. A certain amount of aqueous $RuCl_3$ solution (25 mg/mL) was added into the ethanol dispersion of $Mg(OH)_2$. After stirring for 3 hours, the

products were collected through centrifugation, washed 3 times with ethanol, and dried at 80 °C in a vacuum oven. The dried sample was transferred to a tube furnace and treated at 150°C (Ru-X-150°C) in H_2 atmosphere for 1 hour to obtain the final catalysts. Similar procedures were used to prepare Ru-X-500°C. After the reduction in H_2, Ru-X-500°C was dispersed in water for 12 hours to convert MgO back to $Mg(OH)_2$. Finally, the products were collected through centrifugation and dried at 50 °C in a vacuum oven. For gas-phase photocatalytic tests, samples were prepared by drop casting Ru catalysts powders from an aqueous dispersion onto 1 inch by 1 inch binder free borosilicate glass microfiber filters (Whatman, GF/F, 0.7 μm).

1.4 Characterization

The studies of sample morphology and structure, high-angle annular dark field scanning transmission electron microscopy (HAADF-STEM) image and EDS elemental mappings were performed by a FEI TECNAI F20 transmission electron microscope operating at 200 KV. SEM studies were acquired by scanning electron microscopy (Zeiss, Gemini 500). The SEM samples were prepared by dropping ethanol dispersions of the samples onto Si substrates and then evaporating at room temperature. The Brunauer– Emmett–Teller (BET)

data were collected from a Micromeritics ASAP 2050 machine from Micromeritics, United States. Diffuse reflectance spectra were obtained using a Lambda 950 UV/VIS/NIR spectrometer from Perkin Elmer equipped with an integrating sphere with a diameter of 150 mm. The powder XRD was measured by an Empyrean diffractometer with the Cu Ka radiation. XPS was performed using a ThermoFischer，ESCALAB 250Xi spectrometer with an Al Ka X-ray source operating at 15 kV. The Ru content of different samples were measured by an inductively coupled plasma source mass spectrometer (ICP-MS) (Aurora M90, Jenoptik). Temperature-programmed hydrogen reduction (H_2-TPR) was performed in an apparatus with a Thermo Scientific Nicolet Is 50 fourier transform infrared spectrometer detector.

1.5 Gas-Phase Photothermal catalytic Measurements.

The gas-phase photothermal catalytic experiments were conducted in a batch reactor with internal gas circulation. The pressure inside the reactor was monitored during the reaction using an MIK-P300 pressure transducer. A 300-W Xe arc lamp was used to illuminate the catalysts without any filter. The reactor was degassed and purged with a mixture of CO_2 and H_2 (1:1) twice. The reactor was then sealed when the pressure inside reached 1 bar, and the light was turned on to initiate the photocatalytic reaction. The amounts of gas

products (CO and CH_4) were analyzed with a flame ionization detector (FID) installed in a GC-7900 gas chromatograph (GC) (TECHCOMP).

2 Supplementary Figures and Table

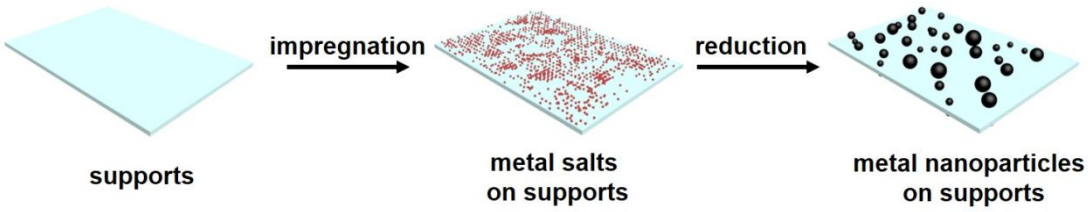

Figure S1. Schematic illustration of conventional impregnation method route to supported nanoparticles catalysts.

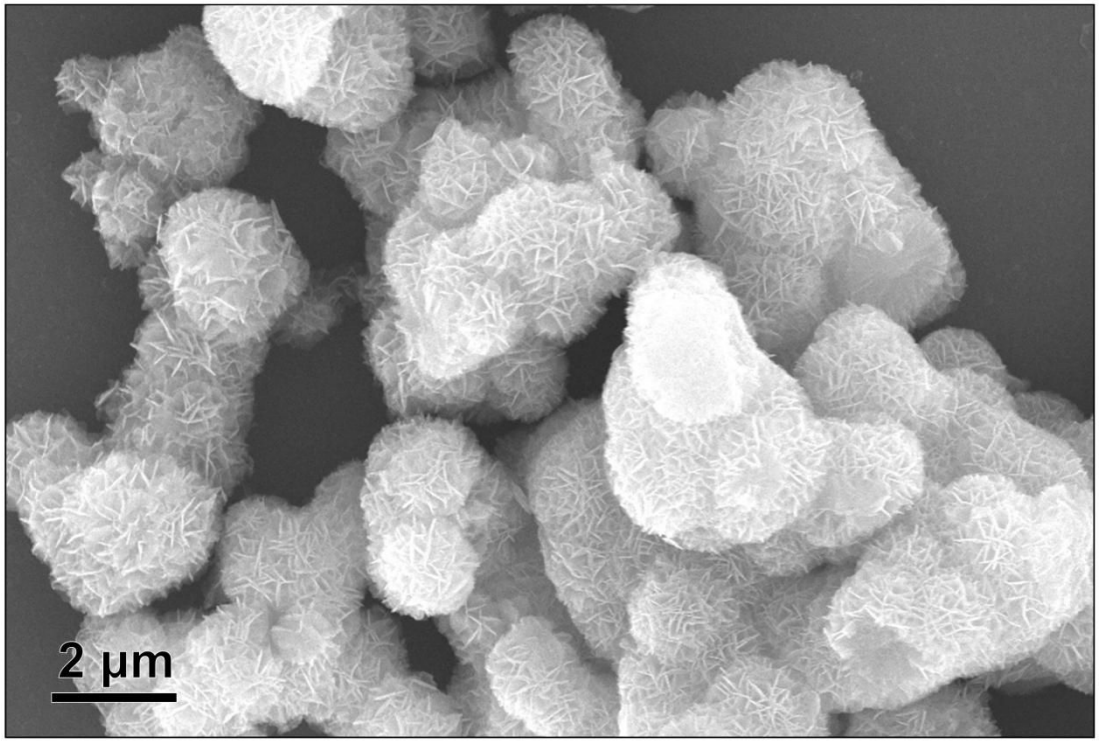

Figure S2. SEM image of the flowerlike $Mg(OH)_2$ support.

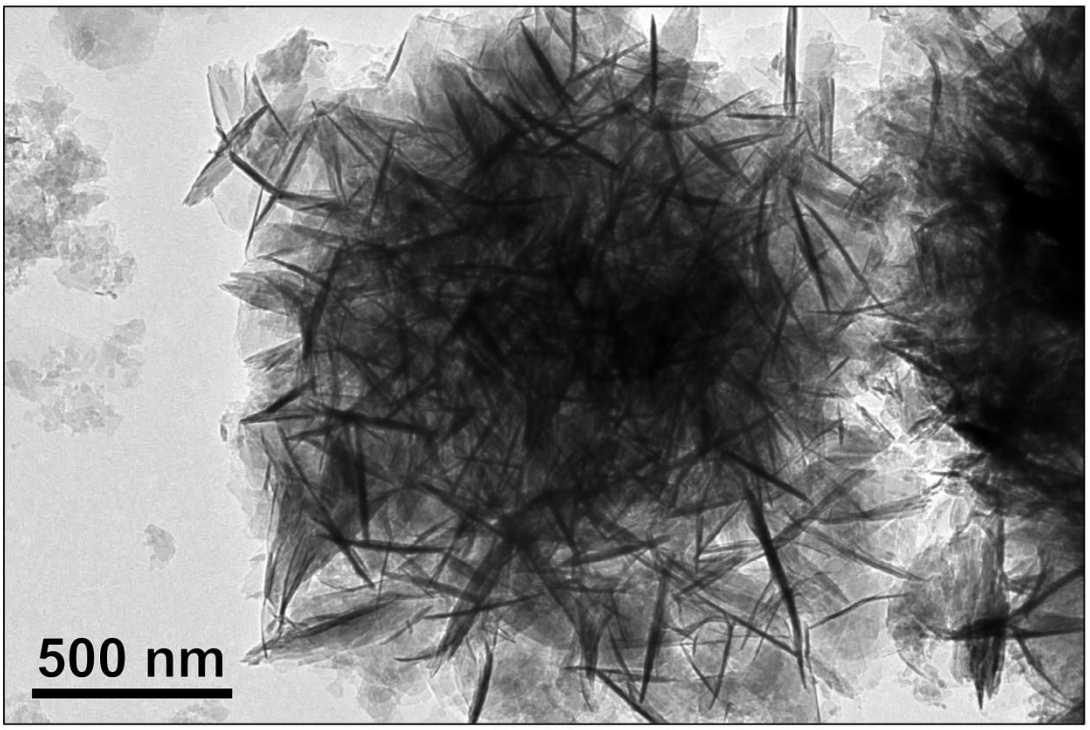

Figure S3. TEM image of the $Mg(OH)_2$ support consisting of interlaced $Mg(OH)_2$ nanoflakes with the thickness about 10 nm.

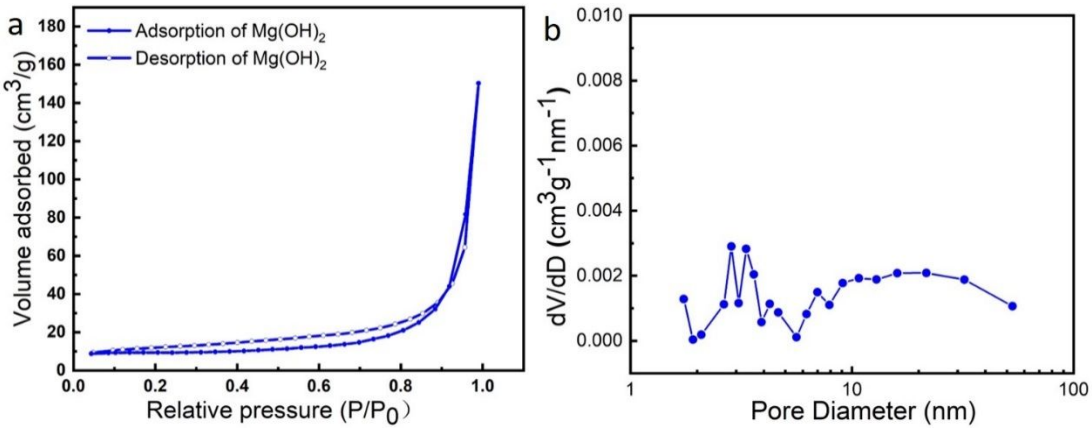

Figure S4. (a) N_2 adsorption-desorption isotherms and (b) the corresponding pore size distribution of $Mg(OH)_2$.

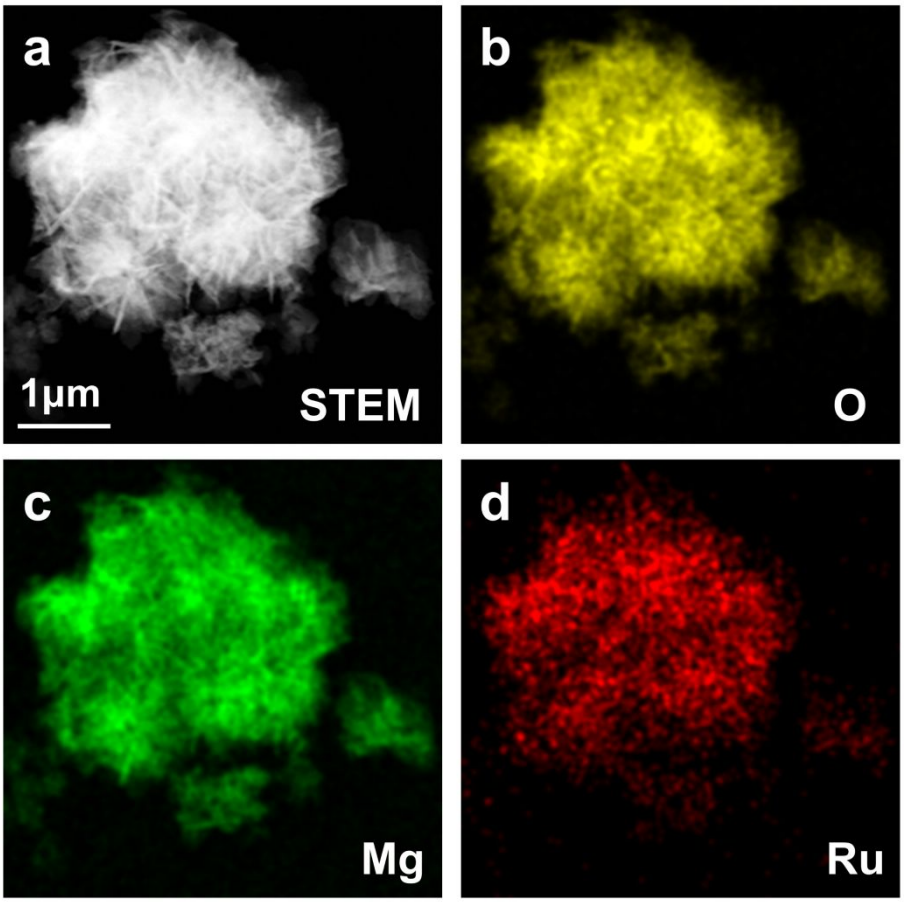

Figure S5. STEM and element mapping images of $Ru(OH)_{3+x}/Mg(OH)_2$.

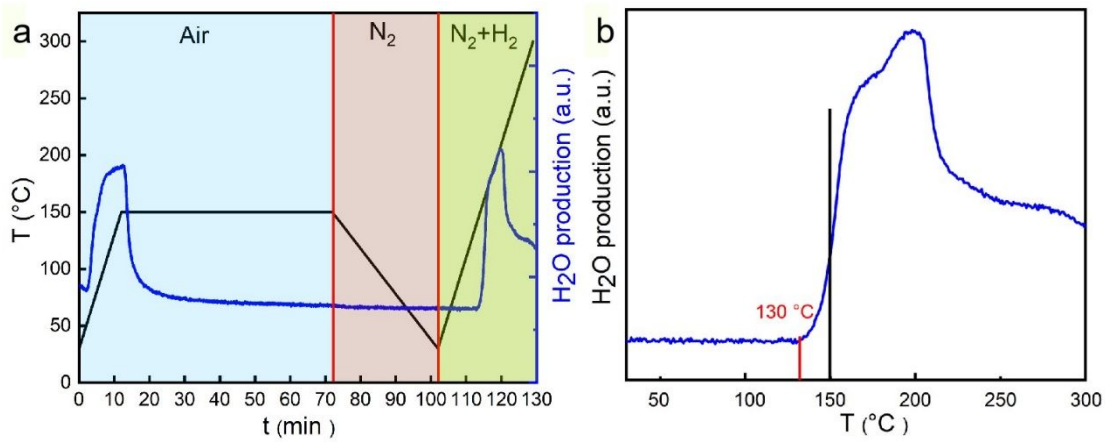

Figure S6. (a) Time-dependent H_2O production profile (blue curve) of $Ru(OH)_{3+x}/Mg(OH)$. The conditions of the H_2-TPR experiment were illustrated by the time-dependent temperature profile (black curve) and background colors corresponding to different gas atmosphere. (b) H_2-TPR profile obtained from the third region (H_2 : N_2 = 1:1).

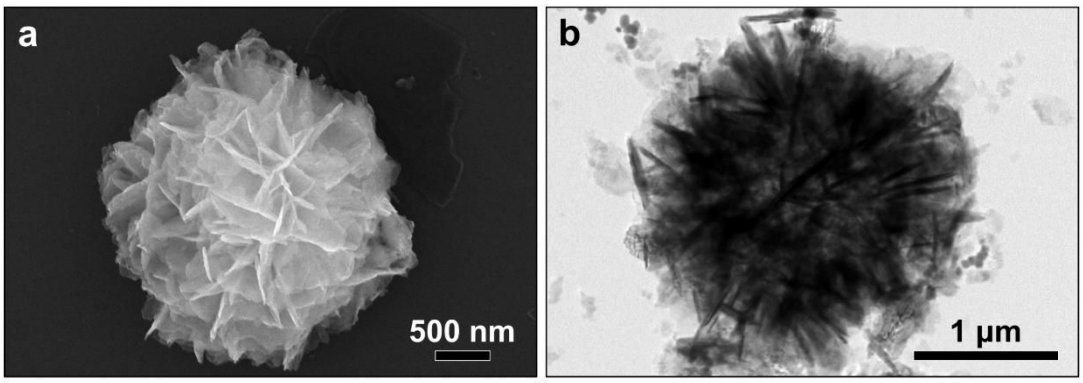

Figure S7. (a) SEM and (b) TEM images of Ru-8.3-150°C. The morphology of self-supported structures was well preserved.

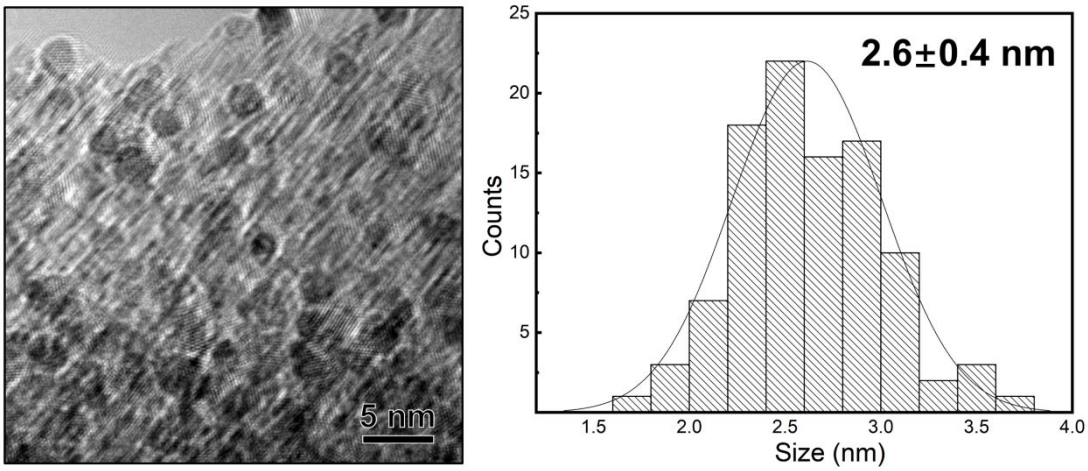

Figure S8. HRTEM image and the Ru particle size distribution of Ru-8.3-150°C.

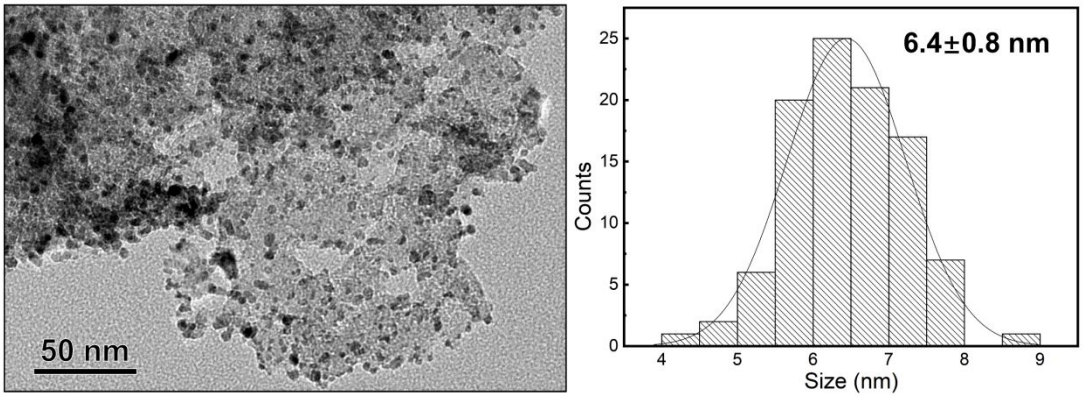

Figure S9. TEM image and the Ru particle size distribution of Ru-7.7-500°C.

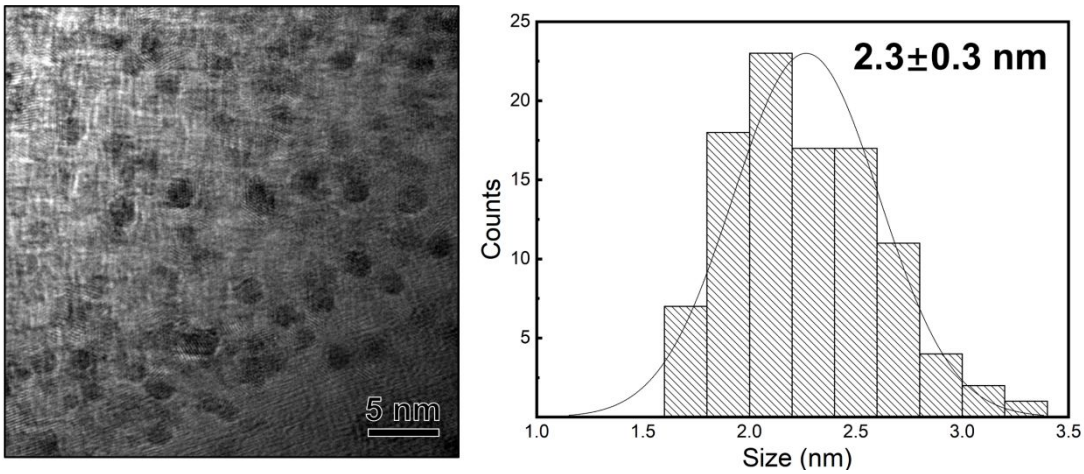

Figure S10. HRTEM image and the Ru particle size distribution of Ru-1.0-150°C.

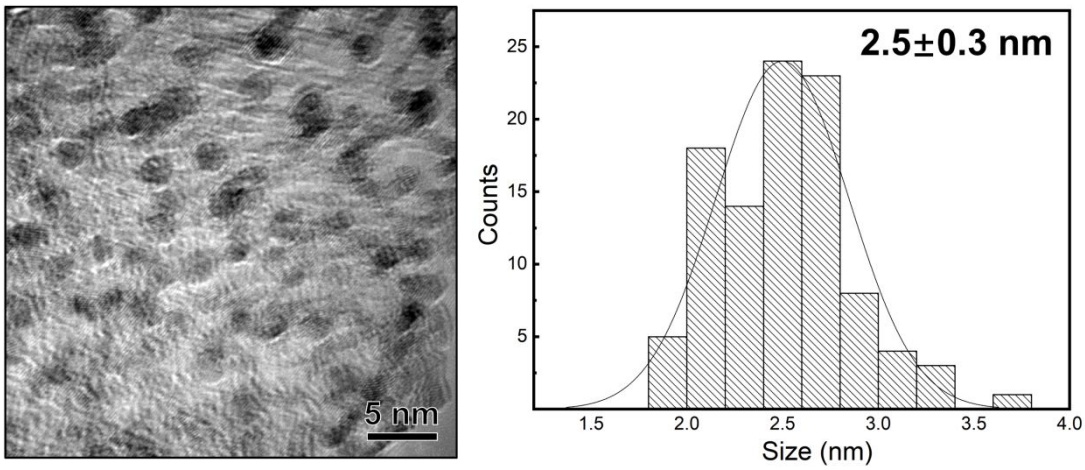

Figure S11. HRTEM image and the Ru particle size distribution of Ru-3.2-150°C.

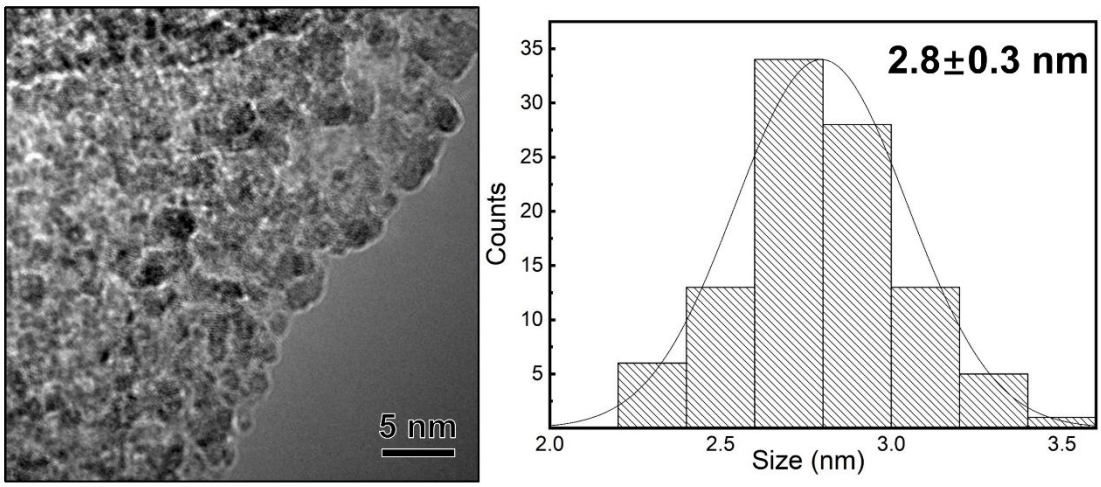

Figure S12. HRTEM image and the Ru particle size distribution of Ru-11.5-150°C.

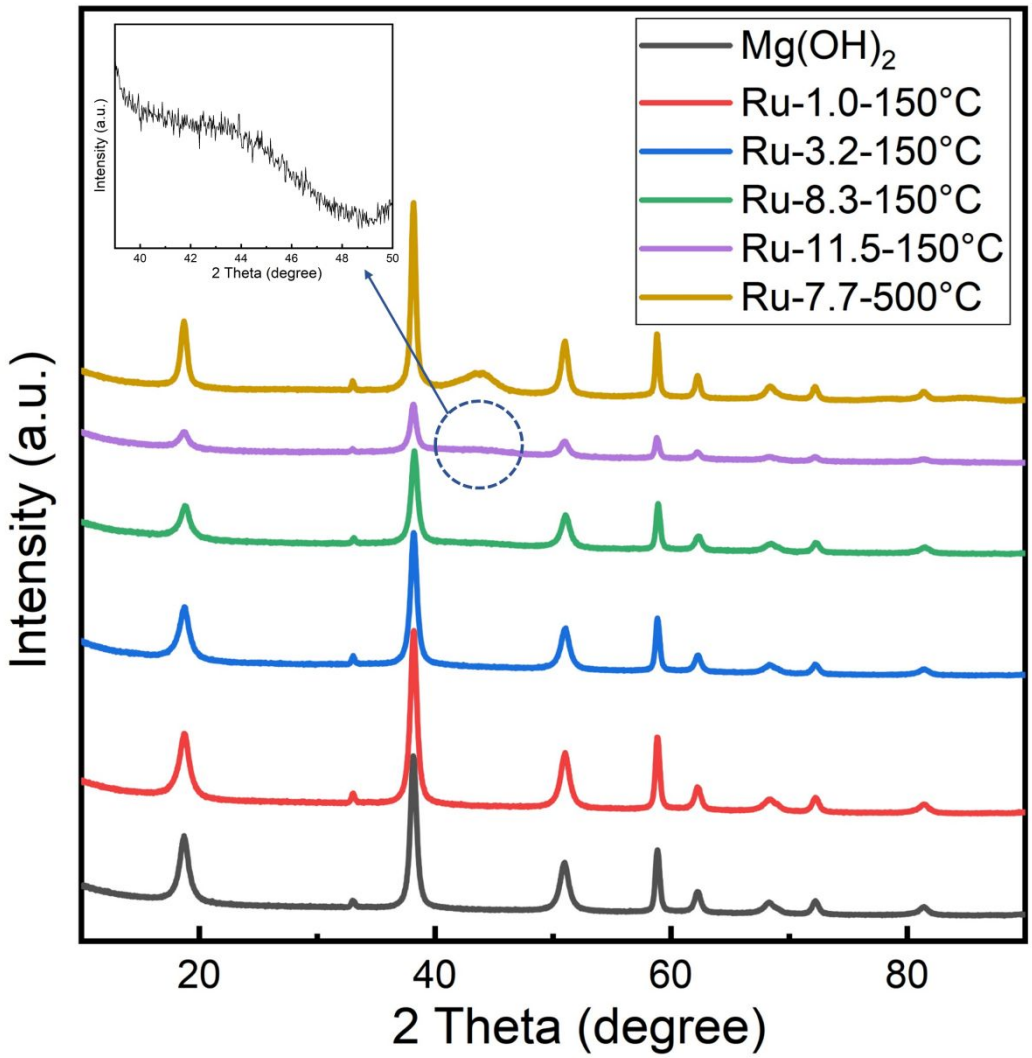

Figure S13. XRD patterns of the $Mg(OH)_2$ support and different Ru catalysts. Inset shows an enlarged region in the curve of Ru-11.5-150°C.

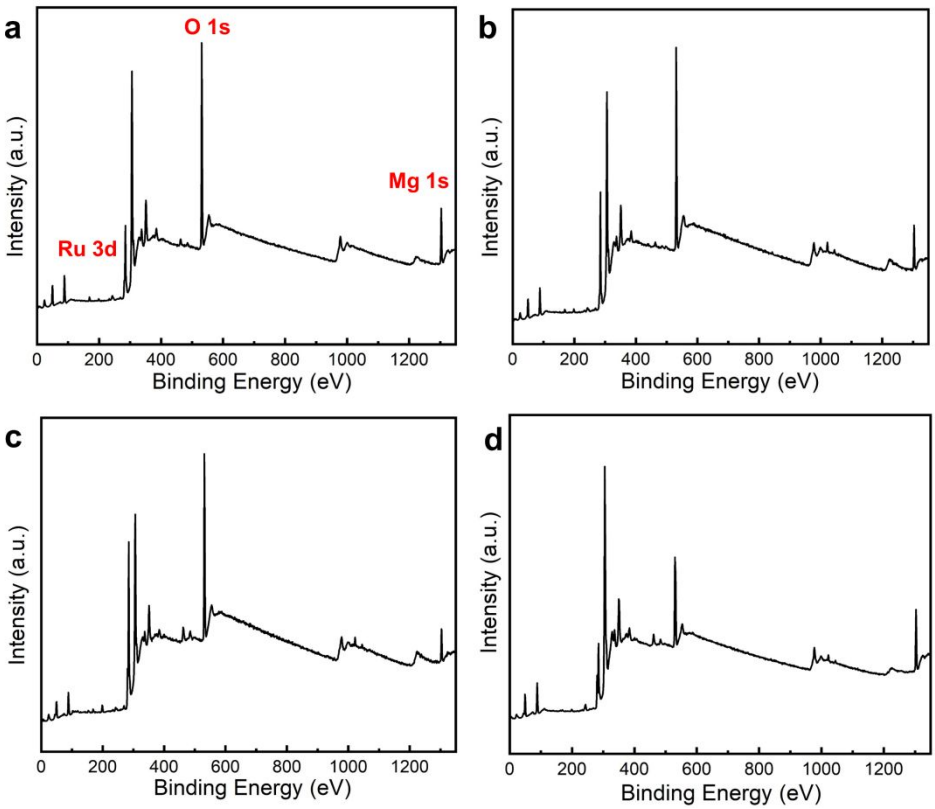

Figure S14. Full XPS spectra of (a) Ru-3.2-150°C, (b) Ru-8.3-150°C, (c) Ru-11.5-150°C and (d) Ru-7.7-500°C.

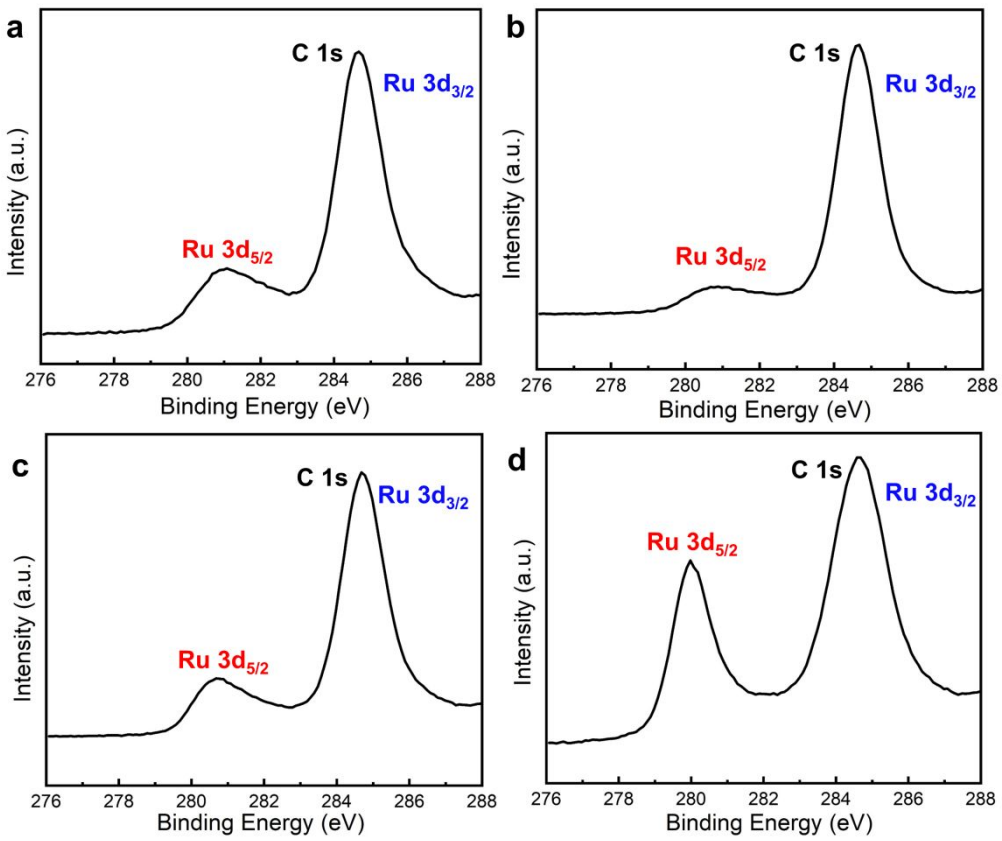

Figure S15. Ru 3d core-level XPS spectra of (a) Ru-3.2-150°C, (b) Ru-8.3-150°C, (c) Ru-11.5-150°C and (d) Ru-7.7-500°C.

Table S1. Ru($3p_{3/2}$) and ($3d_{5/2}$) binding energies of these Ru catalysts.

Sample	Ru ($3p_{3/2}$)/eV	Ru ($3d_{5/2}$)/eV
Ru-3.2-150°C	462.6	281.0
Ru-8.3-150°C	462.4	280.6
Ru-11.5-150°C	462.3	280.7
Ru-7.7-500°C	461.4	280.0
Ru[a]	461.70	279.75
RuO_2[a]	463.2	281.37

[a]The binding energy data of Ru and RuO_2 were obtained from Surf. Interface Anal. 2015, 47, 1072–1079.

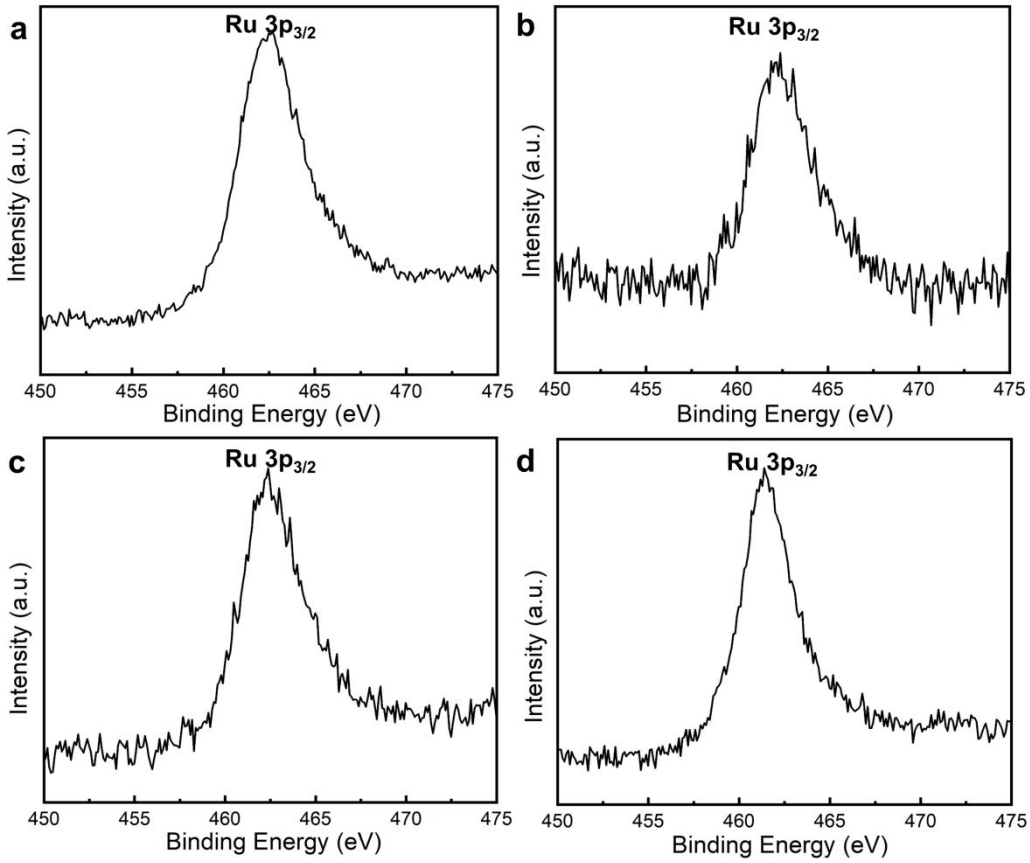

Figure S16. Ru 3p core-level XPS spectra of (a) Ru-3.2-150°C, (b) Ru-8.3-150°C, (c) Ru-11.5-150°C and (d) Ru-7.7-500°C.

Table S2. The number of active sites of different samples estimated by the CO pulse adsorption method based on an assumption that CO was adsorbed on the surface of semi-spherical Ru particles at CO/(surface Ru atom) ratio of 1/1.

Sample	Active sites ($\mu mol/g_{cat}$)
Ru-1.0-150°C	0.0089
Ru-3.2-150°C	0.024
Ru-8.3-150°C	0.062
Ru-7.7-500°C	0.037

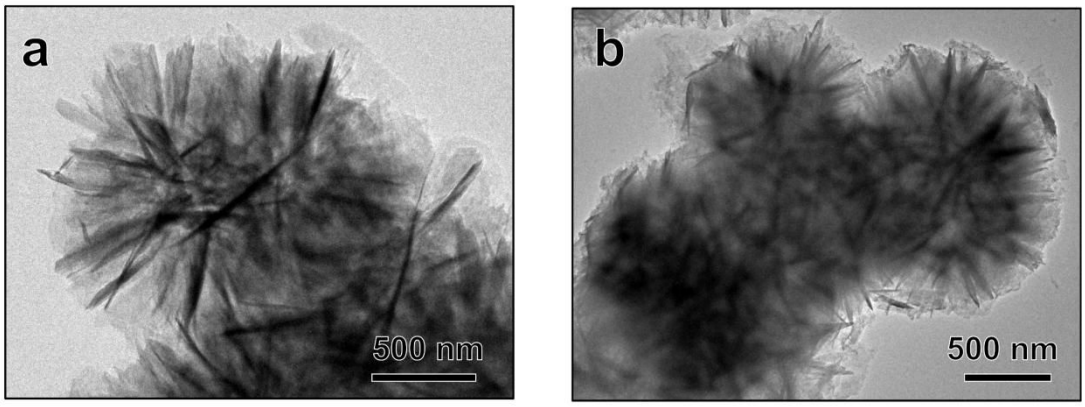

Figure S17. TEM images of Ru-8.3-150°C catalysts (a) before and (b) after the photothermal catalytic testing.

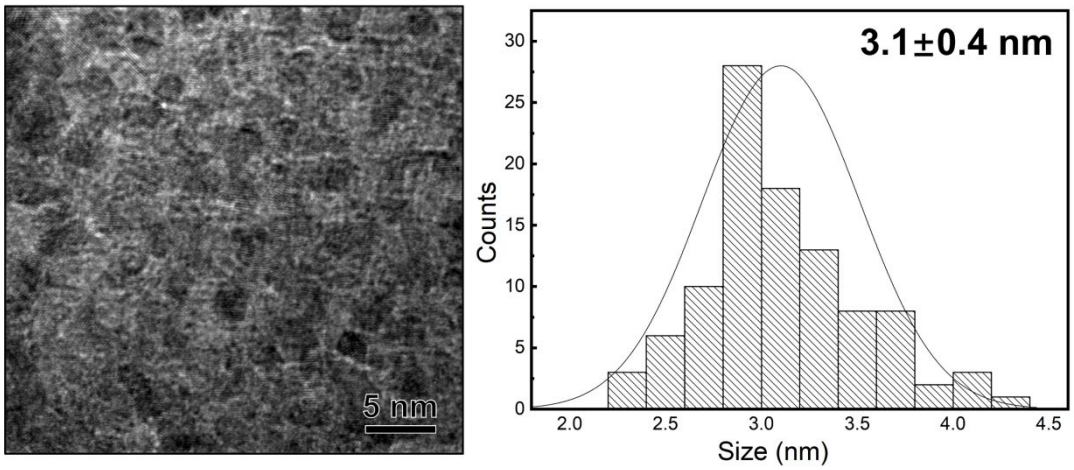

Figure S18. HRTEM image and the Ru particle size distribution of Ru-8.3-150°C after 7 catalytic cycles.

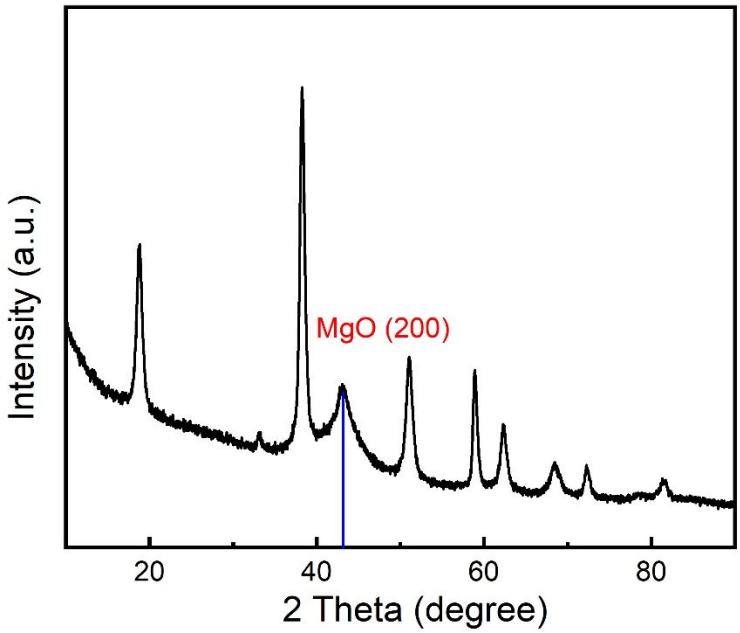

Figure S19. XRD pattern of Ru-8.3-150°C after 7 catalytic cycles.

Table S3. Comparison of the catalytic performance.

Catalyst	Rate	Light intensity (Sun)	Reaction gas (H_2:CO_2)	Reference
Ru/$Mg(OH)_2$	545mmol/h/g	18	1:1	This study
Ru/Al_2O_3	18.16mol/h/g	Not mentioned	4:1	1
Ru/MgAl-LDH	277mmol/h/g	10	4:1	2
Ru/Silicon nanowire	0.99mmol/h/g	3.2	4:1	3
Ru/i-Si-o	2.8mmol/h/g	24.7	4:1	4
RuO_2/silicon photonic crystal	4.4mmol/h/g	22	4:1	5
Pd/Nb_2O_5	1.8mmol/h/g	25	1:1	6

The performance of photothermal hydrogenation is affected by several experiment conditions, such as reactor design, light source and CO_2/H_2 ratio. It is of no practical significance to directly compare the catalytic activities in each work. And the selectivity of Ru catalysts is also affected by the CO_2/H_2 ratio. In this study, a 1:1 CO_2/H_2 ratio instead of 1:4 (in many references) was used. The feeding of more H_2 will favors the further hydrogenation of CO to methane.

Reference:

(1) Meng, X.; Wang, T.; Liu, L.; Ouyang, S.; Li, P.; Hu, H.; Kako, T.; Iwai, H.; Tanaka, A.; Ye, J., Photothermal conversion of CO_2 into CH_4 with H_2 over group VIII nanocatalysts: an alternative approach for solar fuel production. *Angew. Chem. Int. Ed.* **2014,** *53* (43), 11478-82.

(2) Ren, J.; Ouyang, S.; Xu, H.; Meng, X.; Wang, T.; Wang, D.; Ye, J., Targeting activation of CO_2 and H_2 over Ru-loaded ultrathin layered double hydroxides to achieve efficient photothermal CO_2 methanation in flow-type system. *Adv. Energy Mater.* **2017,** *7* (5), 1601657.

(3) O'Brien, P. G.; Sandhel, A.; Wood, T. E.; Jelle, A. A.; Hoch, L. B.; Perovic, D. D.; Mims, C. A.; Ozin, G. A., Photomethanation of gaseous CO_2 over Ru/silicon nanowire catalysts with visible and near-infrared photons. *Adv. Sci.* **2014,** *1* (1), 1400001.

(4) O'Brien, P. G.; Ghuman, K. K.; Jelle, A. A.; Sandhel, A.; Wood, T. E.; Loh, J. Y. Y.; Jia, J.; Perovic, D.; Singh, C. V.; Kherani, N. P.; Mims, C. A.; Ozin, G. A.,

Enhanced photothermal reduction of gaseous CO_2 over silicon photonic crystal supported ruthenium at ambient temperature. *Energy Environ. Sci.* **2018,** *11* (12), 3443-3451.

(5) Jelle, A. A.; Ghuman, K. K.; O'Brien, P. G.; Hmadeh, M.; Sandhel, A.; Perovic, D. D.; Singh, C. V.; Mims, C. A.; Ozin, G. A., Highly efficient ambient temperature CO_2 photomethanation catalyzed by nanostructured RuO_2 on silicon photonic crystal support. *Adv. Energy Mater.* **2018,** *8* (9), 1702277.

(6) Jia, J.; O'Brien, P. G.; He, L.; Qiao, Q.; Fei, T.; Reyes, L. M.; Burrow, T. E.; Dong, Y.; Liao, K.; Varela, M.; Pennycook, S. J.; Hmadeh, M.; Helmy, A. S.; Kherani, N. P.; Perovic, D. D.; Ozin, G. A., Visible and Near-Infrared Photothermal Catalyzed Hydrogenation of Gaseous CO_2 over Nanostructured Pd@Nb_2O_5. *Adv. Sci.* **2016,** *3* (10), 1600189.